# Effect of ammonia on methane production pathways and reaction rates in acetate-fed biogas processes

L. P. Hao, L. Mazéas, F. Lü, J. Grossin-Debattista, P. J. He and T. Bouchez

## ABSTRACT

In order to understand the correlation between ammonia and methanogenesis metabolism, methane production pathways and their specific rates were studied at total ammonium nitrogen (TAN) concentrations of 0.14–9 g/L in three methanogenic sludges fed with acetate, at both mesophilic and thermophilic conditions. Results showed that high levels of TAN had significant inhibition on methanogenesis; this could, however, be recovered via syntrophic acetate oxidation (SAO) coupled with Hydrogenotrophic Methanogenesis (HM) performed by acetate oxidizing syntrophs or through Acetoclastic Methanogenesis (AM) catalyzed by Methanosarcinaceae, after a long lag phase >50 d. Free ammonia ($NH_3$) was the active component for this inhibition, of which 200 mg/L is suggested as the threshold for the pathway shift from AM to SAO-HM. Methane production rate via SAO-HM at TAN of 7–9 g/L was about 5–9-fold lower than that of AM at TAN of 0.14 g/L, which was also lower than the rate of AM pathway recovered at TAN of 7 g/L in the incubations with a French mesophilic inoculum. Thermophilic condition favored the establishment of the SAO-catalyzing microbial community, as indicated by the higher reaction rate and shorter lag phase. The operational strategy is thus suggested to be adjusted when $NH_3$ exceeds 200 mg/L.

**Key words** | Acetoclastic Methanogenesis, ammonia, reaction rate, stable carbon isotrope signature, syntrophic acetate oxidation

**L. P. Hao**
Center for Microbial Communities, Department of Chemistry and Bioscience,
Aalborg University,
Aalborg,
Denmark

**L. P. Hao**
**L. Mazéas** (corresponding author)
**J. Grossin-Debattista**
**T. Bouchez**
Irstea, UR HBAN,
1 rue Pierre-Gilles de Gennes,
Antony 92761,
France
E-mail: *laurent.mazeas@irstea.fr*

**F. Lü**
**P. J. He**
State Key Laboratory of Pollution Control and Resource Reuse,
Tongji University,
Shanghai,
China

## INTRODUCTION

Anaerobic digestion (AD) process is an important technology for the production of renewable energy in the form of $CH_4$ from organic waste streams (De Vrieze *et al.* 2012; Narihiro *et al.* 2015). In this process, energy-rich methane is mainly generated from acetate and $H_2/CO_2$ through Acetoclastic (AM) and Hydrogenotrophic Methanogenesis (HM) as catalyzed respectively by acetotrophic and hydrogenotrophic methanogens. Acetoclastic activity has always been generally considered to be the dominant pathway (Zinder & Koch 1984). In the past decade, a second metabolism was reported for the formation of $CH_4$ from acetate precursor, that occurs via syntrophic acetate oxidation (SAO) in which acetate is oxidized to $H_2$ and $CO_2$ by acetate oxidizing bacteria, followed with consumption of $H_2/CO_2$ by the hydrogenotrophs (SAO-HM). SAO has been found in anaerobic digesters with diverse environments, especially under high ammonia concentrations (Karakashev *et al.* 2006; Westerholm *et al.* 2011; Sun *et al.* 2014; Werner *et al.* 2014; Hao *et al.* 2016), indicating the importance of this pathway and relevant functional microorganisms for commercial biogas production when encountering ammonia inhibition problems.

Total ammonium (in the form of free molecule $NH_3$ and ion $NH_4^+$) can be a methanogenesis inhibitor when accumulated to high concentrations (up to tens of g/L) in AD of nitrogen-rich wastes (Westerholm *et al.* 2011; Westerholm 2012; Fotidis *et al.* 2013a, 2013b; Lv *et al.* 2014). The toxicity has been ascribed to proton imbalance and/or potassium deficiency induced by diffusion of $NH_3$ into cells (Westerholm 2012). The bioprocess can be sometimes deteriorated due to the interaction between ammonium, acids and pH, or in some cases an ‘inhibited pseudo-steady state’ may appear, a condition where the process is running stably but with a lower methane yield (Chen *et al.* 2008; Lü *et al.* 2013).

In the biogas processes, various functional microbes and pathways demonstrated different responses to ammonia stress. Generally, acetotrophic methanogens are considered

doi: 10.2166/wst.2017.032

to be less tolerant than the hydrogenotrophic ones (Chen *et al.* 2008; Demirel & Scherer 2008). The opposite was, however, also reported (Wiegant & Zeeman 1986; Fujishima *et al.* 2000). Considering the SAO metabolism, $NH_4^+$-N ≥ 3 g/L was suggested to initiate the activity of acetate oxidizing syntrophs (Schnürer & Nordberg 2008), as a shift of predominant pathway from AM to HM occurred with elevated $NH_4^+$-N concentration. Behavior of the versatile Methanosarcinaceae under ammonia stress is still a 'mystery'. AM activity performed by its members was observed at 5–7 g/L of $NH_4^+$-N (Lü *et al.* 2013; Fotidis *et al.* 2013a; Hao *et al.* 2015). However, $H_2/CO_2$ utilization or even acetate oxidation by this methanogen family cannot be excluded (De Vrieze *et al.* 2012; Lü *et al.* 2013). The threshold of $NH_4^+$ and $NH_3$ concentration as a warning of methanogenesis inhibition or pathway shift is therefore important for digester operators to take efficient measure. A clear relationship between $NH_3$ concentration and methanogenic pathways/reaction rates is, however, still lacking in previous studies.

Temperature is another factor that can significantly influence the microbial community structure and methanogenic pathways (De Vrieze *et al.* 2015). Thermophilic conditions can favor hydrogenotrophic methanogens, but not Methanosaetaceae (Demirel & Scherer 2008). Although acetate-oxidizing bacteria were found under both mesophilic and thermophilic conditions (Hattori 2008; Westerholm 2012), higher temperature is energetically favorable to the SAO reaction (Hattori 2008), which has been established as a predominant pathway in several thermophilic digesters (Zinder & Koch 1984; Karakashev *et al.* 2006; Sun *et al.* 2014). Furthermore, a fraction of $NH_3$ can increase with elevated temperature (Chen *et al.* 2008), that may also influence the inhibitory effect of ammonia on methanogenesis. Thus, a detailed link between $NH_3$, the contribution of various pathways and functional microorganisms under both temperature regimes should be studied in order to relieve ammonia stress and optimize biogas production when AD process encounters ammonia inhibition problems.

In this study, the methane production process was compared in a wide range of total ammonium nitrogen (TAN) concentrations from 0.14 to 9 g/L at thermophilic and mesophilic conditions. Three methanogenic sludges that originated from different anaerobic reactors in China and France were used. The aim was to make proposals for operation of biogas reactors under high ammonia levels by revealing the relationship between methane production pathway, reaction rates, free ammonia concentration and functional microorganisms.

## MATERIALS AND METHODS

### Experimental set-up

Three types of inocula were used for a comparison between thermophilic and mesophilic methanogenic microbiome of different origins: 'TCS' was taken from a thermophilic anaerobic reactor in China treating synthetic 'wastewater' made from glucose and acetate; 'MCS' and 'MFS' originated from two mesophilic anaerobic digesters in China and France, treating industrial wastewater (Table 1; Supplemental Methods, Section 1, available with the online version of this paper). Freshly collected methanogenic sludges were added to 100 mL BMP medium in serum bottles to reach a volatile solids concentration of 4 g/L. TAN concentration was regulated to 0.14, 3.0, 5.0, 7.0 and 9.0 g/L (calculated as $NH_4^+$-N) in different reactors by adding $NH_4Cl$, to induce 'inhibitory effects' of different degrees. Most experiments were conducted in duplicate, while only one reactor was set up for 3.0 g/L of TAN. 100 mmol/L sodium acetate was used as the substrate. The initial pH was adjusted to 7.0 (±0.1) and controlled below 8.0 during the process by adding 1 mol/L HCl solution. Inocula of MCS and MFS were incubated statically at 35 °C and inoculum TCS was incubated at 55 °C (refer to Section 1 in Supplemental Methods for more details).

### Analysis of gaseous samples

Methane yield was calculated by using the gas pressure and gas composition values, which was assimilated to an ideal gas (Hao *et al.* 2015). Gas pressure in the headspace was periodically measured using a differential manometer (Digitron 2082P). Biogas composition was analyzed using a micro GC (CP4900, Varian) equipped with four parallel chromatographic lines (two molecular sieve 5A, one poraplot Q and one volamine columns), coupled with a thermoconductivity detector, as described by Chapleur *et al.* (2014).

Gas samples used for analyzing stable carbon isotope compositions of $CH_4$ ($\delta^{13}CH_4$) and $CO_2$ ($\delta^{13}CO_2$) were collected using a syringe, transferred into 7-mL vacuum serum tubes and stored for isotopic analysis as used previously (refer to Section 3 in Supplemental Methods, available with the online version of this paper). The apparent fractionation factor was calculated by using the following formula (Whiticar *et al.* 1986):

$$\alpha_C = \frac{(\delta^{13}CO_2 + 10^3)}{(\delta^{13}CH_4 + 10^3)} \quad (1)$$

**Table 1** | Set up of reactors using three different inocula

| Reactor | Inoculum | TAN (calculated as $NH_4^+$-N) (mmol/L) | (g/L) | Temperature °C |
|---|---|---|---|---|
| TCS-N0.14 (1) | Thermophilic Chinese sludge (TCS)[a] | 10 | 0.14 | 55 |
| TCS-N0.14 (2) | | 10 | 0.14 | |
| TCS-N3 (1) | | 214 | 3.00 | |
| TCS-N5 (1) | | 357 | 5.00 | |
| TCS-N5 (2) | | 357 | 5.00 | |
| TCS-N7 (1) | | 500 | 7.00 | |
| TCS-N7 (2) | | 500 | 7.00 | |
| TCS-N9 (1) | | 643 | 9.00 | |
| TCS-N9 (2) | | 643 | 9.00 | |
| MCS-N0.14 (1) | Mesophilic Chinese sludge (MCS)[b] | 10 | 0.14 | 35 |
| MCS-N0.14 (2) | | 10 | 0.14 | |
| MCS-N3 (1) | | 214 | 3.00 | |
| MCS-N5 (1) | | 357 | 5.00 | |
| MCS-N5 (2) | | 357 | 5.00 | |
| MCS-N7 (1) | | 500 | 7.00 | |
| MCS-N7 (2) | | 500 | 7.00 | |
| MCS-N9 (1) | | 643 | 9.00 | |
| MCS-N9 (2) | | 643 | 9.00 | |
| MFS-N0.14 (1) | Mesophilic French sludge (MFS)[c] | 10 | 0.14 | 35 |
| MFS-N0.14 (2) | | 10 | 0.14 | |
| MFS-N3 (1) | | 214 | 3.00 | |
| MFS-N5 (1) | | 357 | 5.00 | |
| MFS-N5 (2) | | 357 | 5.00 | |
| MFS-N7 (1) | | 500 | 7.00 | |
| MFS-N7 (2) | | 500 | 7.00 | |
| MFS-N9 (1) | | 643 | 9.00 | |
| MFS-N9 (2) | | 643 | 9.00 | |

[a]Originated from a laboratory-scale anaerobic sequenced batch reactor in China, thermophilic, treating synthetic wastewater made from glucose and acetate.
[b]Collected from an industrial upflow anaerobic sludge blanket (UASB) reactor, mesophilic, treating paper mill wastewater in China.
[c]Taken from a full-scale UASB in France, mesophilic, treating effluent from sugar beet industry.

## Analysis of liquid samples

Liquid samples were taken using a sterile syringe and centrifuged at 16,000 g for 5 min (at 4 °C). Supernatant was separated and stored at −20 °C. Acetate concentration in the supernatant was measured by conductimetric detection, using a Dionex 120 ion chromatography system equipped with an IonPac ICE-AS1 analytical column. Dissolved organic carbon was detected by using a BIORITECH 700 analyzer (Bioritech, France). pH was measured immediately after sampling using a Mettler Inlab 427 probe (Mettler Toledo Ltd).

The concentration of free ammonia ($NH_3$) was calculated as described previously (Hao *et al.* 2015) by using the following equation:

$$NH_3 = \frac{17 \times 10^{pH}}{14 \times \exp\left(\frac{6334}{273 + T(^{o}C)}\right) + 10^{pH}} \times TAN \qquad (2)$$

where T represents the temperature (Anthonisen *et al.* 1976).

## Calculation of instant $CH_4$ production rate

The instant $CH_4$ production rate ($R_{CH4}$) was calculated from the measurements of $CH_4$ accumulation, using Origin Pro 10.1 (Origin Lab Corp, USA). The specific methane production rate ($\mu_{CH4}$) was calculated as mol-$CH_4$ produced from per mol acetate added per day [mol/(mol-acetate·d) or $d^{-1}$], obtained from dividing the $R_{CH4}$ by the total amount of acetate initially added. The 'instant' lag phase was defined as the time to the first observation of methane production exceeding 1% in the headspace of the bottles.

## Data fitting to the modified Gompertz model

The modified Gompertz three-parameter model (Zwietering *et al.* 1990) was fitted to the experimentally observed cumulative $CH_4$ production curves, to determine the maximum $CH_4$ production rate ($R_{max}$) and the lag phase ($\lambda$) by using the following equation:

$$M(t) = P \cdot \exp\left\{-\exp\left[\frac{R_{max} \cdot e}{P}(\lambda - t) + 1\right]\right\} \qquad (3)$$

where M(t) is the cumulative $CH_4$ production (mmol $CH_4$) at time t; $P$ is the maximum $CH_4$ potential (mmol $CH_4$) at the end of incubation; $t$ is the time (d); $R_{max}$ is the maximum $CH_4$ production rate [mol $CH_4$/(mol-acetate·d)]; $\lambda$ is the lag phase (d) and $e$ is exp, i.e. 2.71828. The three parameters $P$, $R_{max}$ and $\lambda$ were estimated by curve-fitting using Sigmaplot version 10.0.

## Fluorescence *in situ* hybridization

Fluorescence *in situ* hybridization (FISH) was performed as described by Qu *et al.* (2009), using probes EUB338, ARC915, MX825, MS1414 and MG1200 to respectively target bacteria, archaea, Methanosaetaceae, Methanosarcinaceae and Methanomicrobiales. Detailed probes information, sample fixation and hybridization procedure are described in Section 2 of Supplemental Methods (available with the online version of this paper).

## RESULTS AND DISCUSSION

### Shift of methane production pathways along with increasing TAN

Figure 1(a)–1(c) illustrate the $CH_4$ production curves during the 110 d incubation. Results showed that the inhibitory effect of ammonia on methanogenesis increased with increasing TAN level, as indicated by the longer lag phase and lower methane production rates at elevated TAN levels in all three inocula.

To better characterize $CH_4$ production activities at various ammonia concentrations, the whole process can be divided into three phases according to the instant methane production rate ($\mu_{CH4}$), which were: lag phase ($0 \le \mu_{CH4} < 0.002\ d^{-1}$), slow $CH_4$ production phase ($0.002\ d^{-1} \le \mu_{CH4} \le 0.010\ d^{-1}$) and fast $CH_4$ production phase ($\mu_{CH4} > 0.010\ d^{-1}$). Three $CH_4$ production patterns can be then described: (1) at relatively low TAN levels (0.14–3 g/L for MCS and MFS, 0.14–5 g/L for TCS), $CH_4$ was quickly produced after a short initial lag phase (<10 d); (2) at higher TAN levels (5 g/L for MCS and MFS, 7 g/L for TCS), a second lag or slow $CH_4$ production phase appeared between the two fast $CH_4$ production phases, indicating unstable and inhibited methanogenesis at these 'breakthrough' TAN concentrations; (3) at quite high TAN levels (7 g/L of TAN for MCS and MFS, 9 g/L of TAN for TCS), $CH_4$ was actively produced after a long initial lag phase (>50 d). At 9 g/L of TAN for MCS and MFS, active methanogenesis only started after a lag phase >80 d, which is much longer than that for TCS. It suggested slower activity recovery or growth of ammonia-tolerant microbes under mesophilic conditions. This regular pattern, as demonstrated by $CH_4$ curves, was also observed for the change of acetate and inorganic-carbon dissolved in the liquid phase (Figure S1, available with the online version of this paper).

The dynamics of methane production pathways were evaluated by stable carbon isotopic signature of biogas (Figure 1(d)–1(l)). $\alpha c$ and $\delta^{13}CH_4$ act as pathway indicators, with $\alpha c$ <1.055, $\delta^{13}CH_4 > -60‰$ suggesting predominance of AM pathway; and $\alpha c > 1.065$, $\delta^{13}CH_4 < -60‰$ representing predominance of HM pathway (Whiticar et al. 1986), which has been applied in previous studies (Qu et al. 2009; Lü et al. 2013; Leite et al. 2016; Vaughn et al. 2016). As acetate was used as the only organic substrate, a predominance of HM pathway also indicates active SAO reaction for decomposition of acetate to $CO_2$ and $H_2$.

Results showed that, generally, higher TAN concentrations led to stronger carbon isotope fractionation effect as demonstrated by the increasing divergence between the values of $\delta^{13}CO_2$ and $\delta^{13}CH_4$, and the calculated $\alpha c$ values. Methane production pathway gradually shifted to SAO-HM from AM when TAN reached 7 g/L for MCS and 9 g/L for TCS, since the pathway indicator $\alpha c$ increased to >1.065 therein from <1.055 at lower TAN levels. Closely contacted bacteria and Methanomicrobiales appeared in the fast methane production phase under these conditions (Figure 2(a)–2(b)), which can be speculated to be acetate oxidizing syntrophs. However, the behavior of the MFS-inoculated microbiome was different, as AM activity gradually recovered at 7 g/L of TAN, and many Methanosarcinaceae clusters were observed during the fast methane production period (Figure 2(c)). To the contrary, at TAN of 0.14 g/L, only acetotrophic Methanosaetaceae or Methanosarcinaceae were observed in the microbiome from three inocula (Figure 2(d)–2(f)). It suggested that high TAN levels inhibited the initial AM activity; methanogenesis can, however, initiate after a long lag phase via SAO-HM pathway performed by the syntrophs, or that AM pathway can be recovered as was catalyzed by Methanosarcinaceae.

An intermediate lag was observed between two active methane production phases for MCS, MFS at TAN of 5 g/L and TCS at 7 g/L, which indicated increasing inhibitory effects on methanogenesis under an unchanged TAN level before it recovered. After this lag phase, the predominant pathway shifted to HM as the value of $\alpha c$ gradually increased to $\ge$1.065 (Figure 1(d)–1(f)). It can be speculated that the increasing inhibitory effect result from the increasing $NH_3$ concentration (Figure 3(d)–3(f)) which was induced by the elevated pH (Figure 3(a)–3(c)) after acetate ion was consumed. $NH_3$ was thus the active component causing inhibition and shift of methanogenic pathways as previously reported (Chen et al. 2008; Schnürer & Nordberg 2008).

### Free ammonia as the critical factor for pathway shift

Figure 4 reveals the relationship between $NH_3$ concentration and stable carbon isotope fractionation effect

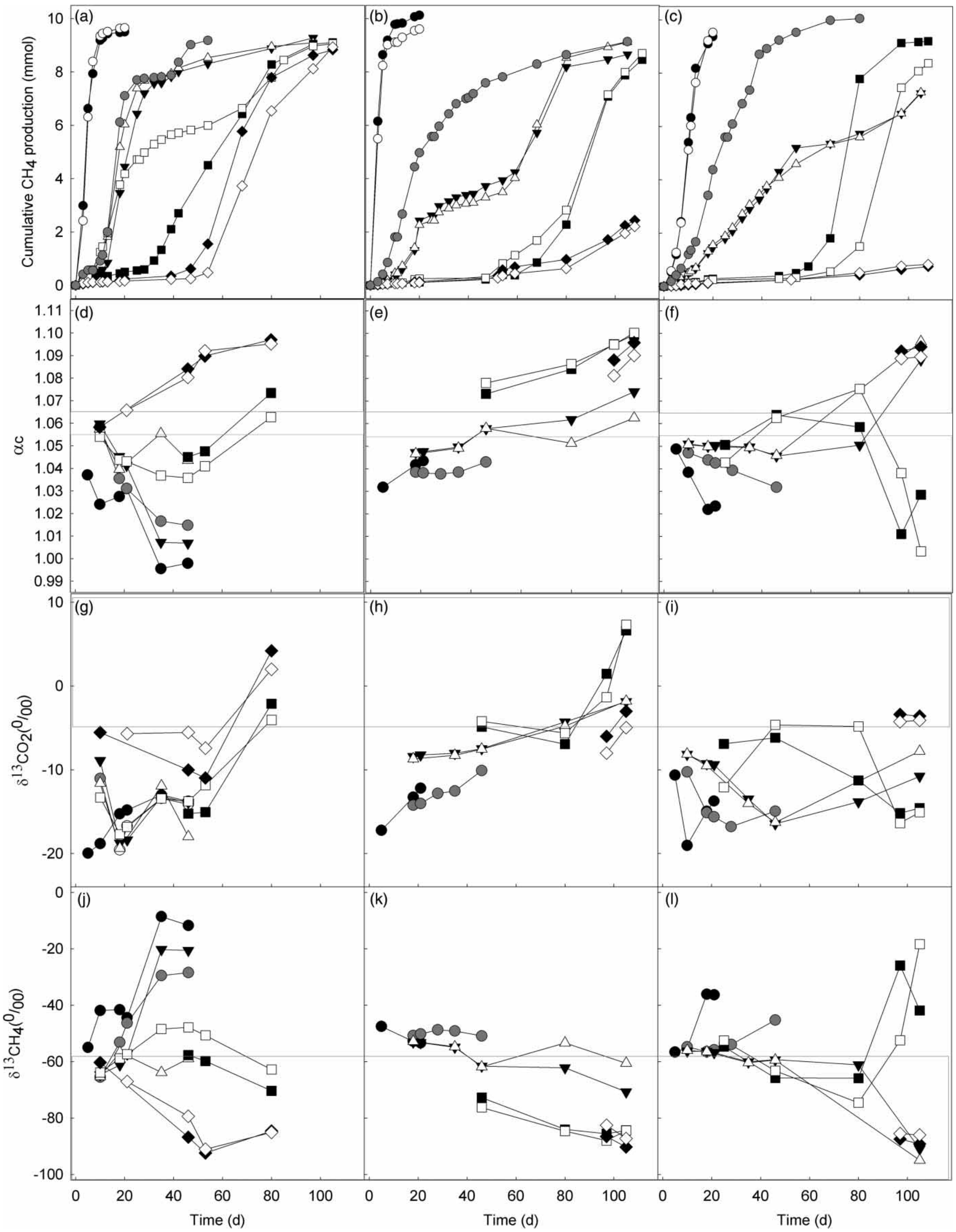


**Figure 1** | Temporal change of cumulative $CH_4$ production (a, b, c), αc (d, e, f), $\delta^{13}CO_2$ (g, h, i) and $\delta^{13}CH_4$ (j, k, l) values for sludge TCS (a, d, g, j), MCS (b, e, h, k), MFS (c, f, I, l) at different ammonia concentrations: ● 0.14 g-N/L, reactor (1); ○ 0.14 g-N/L, reactor (2); ● 3.0 g-N/L, reactor (1); ▼ 5.0 g-N/L, reactor (1); Δ 5.0 g-N/L, reactor (2); ■ 7.0 g-N/L, reactor (1); □ 7.0 g-N/L, reactor (2); ◆ 9.0 g-N/L, reactor (1); ◇ 9.0 g-N/L, reactor (2). Reactors (1) and (2) were operated at the same condition.

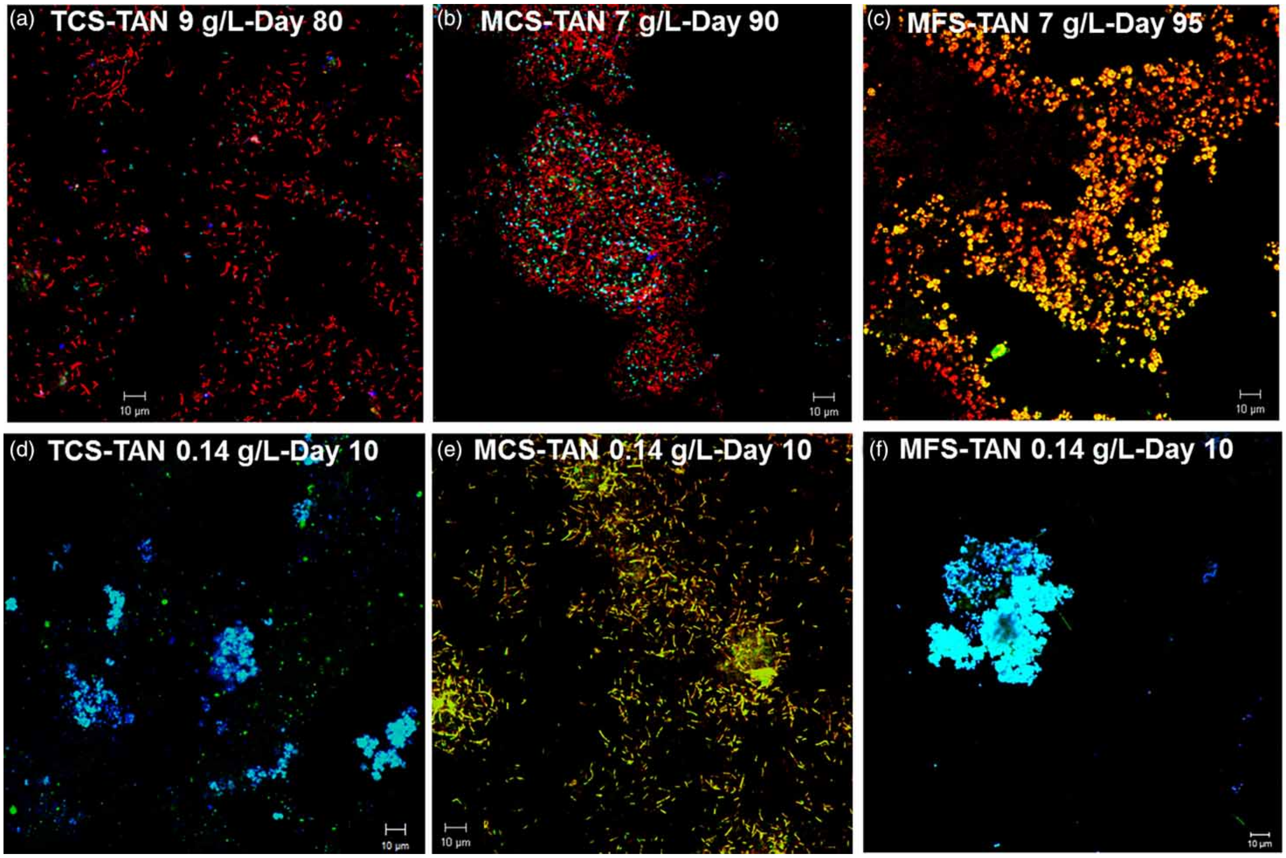


**Figure 2** | FISH photographs at high TAN levels of 9 g/L for TCS (a), 7 g/L for MCS (b) and MFS (c) during fast methane production phase for observation of bacteria (probe EUB338 I, II, III-Cy3, red signal), archaea (probe ARC915-FITC), Methanosacinaceae (probe MS1414-Cy3, yellow signal by overlapping FITC), Methanomicrobiales (probe MG1200-Cy5, light blue signal by overlapping FITC); and at lowest TAN level of 0.14 g/L for TCS (d), MCS (e) and MFS (f) in the end of fast methane production phase for observation of archaea (probe ARC915-FITC), Methanosacinaceae (probe MS1414-Cy5, light blue signal by overlapping FITC) and Methanosaetaceae (probe Mx825-Cy3, yellow signal by overlapping FITC).

during methanogenesis process. Results showed that, under both thermophilic and mesophilic conditions, when $NH_3 \leq$ 200 mg/L, AM pathway predominated as indicated by $\alpha_c <$ 1.055 and $\delta^{13}CH_4 > -60‰$; nevertheless, when $NH_3 >$ 200 mg/L, values of $\delta^{13}CH_4$ and $\delta^{13}CO_2$ changed to be unstable and some of the $\alpha_c$ values became >1.065, which reflected the unstable methanogenic metabolism under inhibited status, and also suggested the shift of dominant pathway to SAO-HM. 200 mg/L was therefore identified as a threshold $NH_3$ level inducing pathway shift under both temperature regimes here, which is in the range of 128–330 mg/L as previously reported for $NH_3$ concentration inhibiting methanogenesis under mesophilic condition (Schnürer & Nordberg 2008).

Surprisingly, AM pathway could still recover at quite high $NH_3$ levels up to 1 g/L in the MFS-inoculated system, as indicated by several $\alpha_c$ values lower than 1.030 under these conditions. It updated the record on the tolerance of acetotrophic Methanosarcinaceae to $NH_3$ (De Vrieze *et al.* 2012).

## Reaction rates of the two pathways for conversion of acetate to methane

Reaction rates of the two methanogenic pathways were compared. SAO-HM demonstrated lower reaction rates than AM pathway at high TAN levels, which was also lower than that of the recovered AM pathway under similar conditions. Thermophilic condition favored SAO-HM compared to mesophilic condition.

Generally, methane production rate quickly decreased with increasing TAN concentration. At breakthrough, TAN levels, the maximum instant rate $\mu_{CH4\text{-}max}$ (appeared in the first fast methane production phase) decreased 6–9-fold (0.012–0.031 $d^{-1}$) compared with that at TAN of 0.14 g/L (Table 2), which expressed the reaction rate for AM before the pathway shift. At maximum TAN levels, $\mu_{CH4\text{-}max}$ for TCS (0.023–0.024 $d^{-1}$) was about one-sixth of that at TAN of 0.14 g/L (0.141–0.149 $d^{-1}$), and for MCS it was one-tenth (0.019–0.020 $d^{-1}$). These values demonstrated the

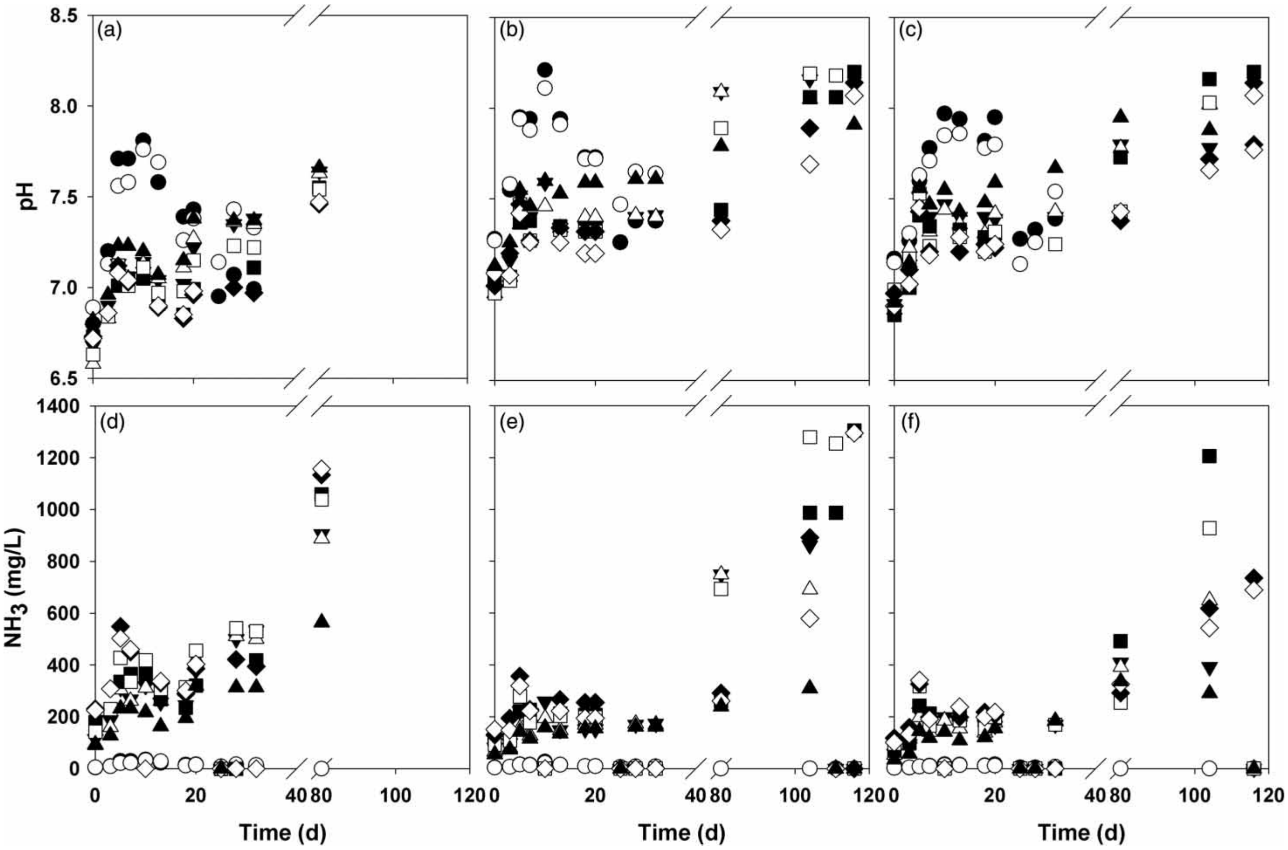

**Figure 3** | Temporal change of cumulative $CH_4$ production (a, b, c), $\alpha$c (d, e, f), $\delta^{13}CO_2$ (g, h, i) and $\delta^{13}CH_4$ (j, k, l) values for sludge TCS (a, d, g, j), MCS (b, e, h, k), MFS (c, f, I, l) at different ammonia concentrations ● 0.14 g-N/L, reactor (1); ○ 0.14 g-N/L, reactor (2); ▲ 3.0 g-N/L, reactor (1); ▼5.0 g-N/L, reactor (1); Δ 5.0 g-N/L, reactor (2); ■ 7.0 g-N/L, reactor (1); □ 7.0 g-N/L, reactor (2); ◆ 9.0 g-N/L, reactor (1); ◇ 9.0 g-N/L, reactor (2). Reactors (1) and (2) were operated at the same condition.

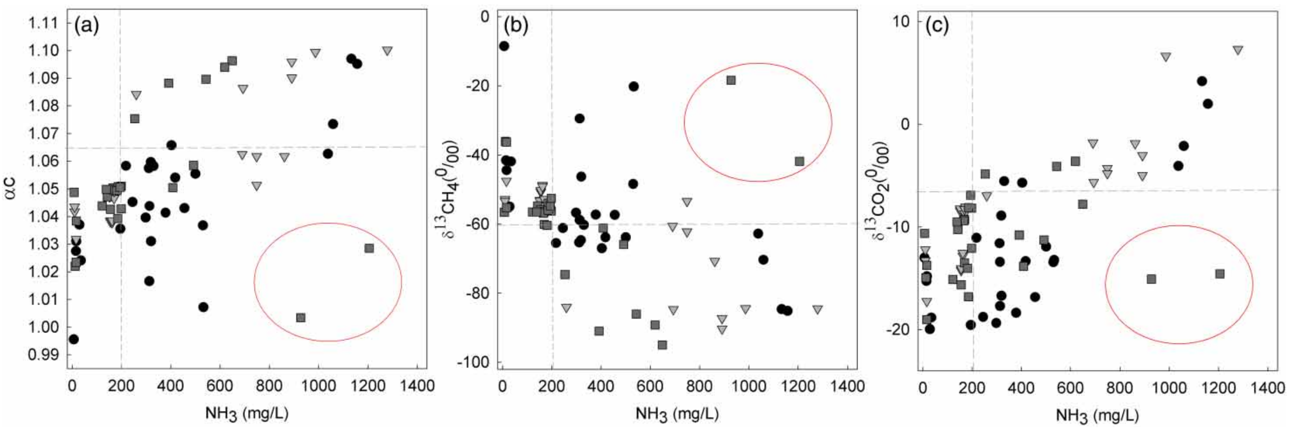

**Figure 4** | Change on values of $\alpha_c$ (d), $\delta^{13}CH_4$ (e), $\delta^{13}CO_2$ (f) along with $NH_3$ concentration for inocula TCS (●), MCS (▲) and MFS (■). Symbols in the circles emphasized isotope signature values which indicate acetoclastic pathway being performed at quite high $NH_3$ levels.

reaction rate of HM which followed the SAO after the pathway shift. At TAN of 7 g/L, $\mu_{CH4\text{-}max}$ for MFS recovered to 0.022–0.031 $d^{-1}$, about one-fourth to one-third of that at TAN of 0.14 g/L (0.091–0.096 $d^{-1}$), displaying AM reaction rates performed by Methanosarcinaceae under different TAN levels.

Methane production curves were fitted to the modified Gompertz model (Table 2), generally, the simulated

**Table 2** | Calculation of maximum instant $CH_4$ production rate and the calculated results using the modified three-parameter Gompertz model for initiation of methanogenesis at different TAN concentrations in three anaerobic sludges. 'NA' means 'not available' in this work

| Reactor | Maximum instant $CH_4$ production rate ($\mu_{CH4\text{-}max}$) mol/(mol-acetate•d) | Maximum $CH_4$ potential ($P$) mmol | Lag phase ($\lambda$) d | Simulated maximum $CH_4$ production rate ($R_{max}$) mol/(mol-acetate•d) | $R^2$ |
|---|---|---|---|---|---|
| TCS-N0.14 (1) | 0.141 | 9.45 | 1.3 | 0.182 | 0.998 |
| TCS-N0.14 (2) | 0.149 | 9.59 | 1.8 | 0.207 | 1.000 |
| TCS-N3 (1) | 0.066 | 8.34 | 9.8 | 0.078 | 0.983 |
| TCS-N5 (1) | 0.053 | 8.57 | 10.7 | 0.047 | 0.992 |
| TCS-N5 (2) | 0.055 | 8.47 | 9.0 | 0.056 | 0.990 |
| TCS-N7 (1) | 0.020 | 10.08 | 27.1 | 0.017 | 0.995 |
| [a]**TCS-N7 (2)** | **0.031** | **5.54** | **6.2** | **0.031** | **0.997** |
| TCS-N9 (1) | 0.024 | 8.95 | 48.7 | 0.031 | 0.998 |
| TCS-N9 (2) | 0.023 | 9.16 | 54.2 | 0.027 | 0.997 |
| MCS-N0.14 (1) | 0.205 | 9.87 | 0.5 | 0.246 | 0.995 |
| MCS-N0.14 (2) | 0.183 | 9.34 | 0.7 | 0.247 | 0.997 |
| MCS-N3 (1) | 0.039 | 8.35 | 3.4 | 0.026 | 0.985 |
| **MCS-N5 (1)** | **0.030** | **3.16** | **8.3** | **0.017** | **0.989** |
| **MCS-N5 (2)** | **0.023** | **3.49** | **9.3** | **0.019** | **0.984** |
| MCS-N7 (1) | 0.020 | 9.87 | 70.2 | 0.020 | 0.993 |
| MCS-N7 (2) | 0.019 | 16.30 | 61.6 | 0.011 | 0.990 |
| MCS-N9 (1) | 0.007 | NA | NA | NA | NA |
| MCS-N9 (2) | 0.006 | NA | NA | NA | NA |
| MFS-N0.14 (1) | 0.096 | 9.79 | 4.4 | 0.101 | 0.994 |
| MFS-N0.14 (2) | 0.091 | 10.22 | 4.1 | 0.089 | 0.997 |
| MFS-N3 (1) | 0.042 | 10.16 | 7.1 | 0.031 | 0.997 |
| **MFS-N5 (1)** | **0.013** | **5.95** | **8.0** | **0.011** | **0.998** |
| **MFS-N5 (2)** | **0.012** | **6.29** | **9.3** | **0.012** | **0.994** |
| MFS-N7 (1) | 0.031 | 9.20 | 64.3 | 0.064 | 0.994 |
| MFS-N7 (2) | 0.022 | 8.56 | 77.0 | 0.047 | 0.995 |
| MFS-N9 (1) | 0.001 | NA | NA | NA | NA |
| MFS-N9 (2) | 0.002 | NA | NA | NA | NA |

[a]Reactors in bold demonstrated instable $CH_4$ production process which included two fast $CH_4$ production periods. Only the first fast $CH_4$ production period was used to fit the modified three-parameter Gompertz model, and the results are shown in Table 2.

maximum methane production rate $R_{max}$ demonstrated similar tendency with $\mu_{CH4\text{-}max}$. The lower methane production rates via SAO agree with previous reports (Karakashev *et al.* 2006; Schnürer & Nordberg 2008), and might explain low biogas production rates in digesters at 'inhibited pseudo-steady state' induced by accumulation of ammonia (Westerholm 2012; Sun *et al.* 2014).

Methane production rates via SAO-HM under thermophilic conditions [$R_{max}$ 0.027–0.031 mol/(mol-acetate·d) for TCS at TAN of 9 g/L] were higher than that under mesophilic conditions [$R_{max}$ 0.011–0.020 mol/(mol-acetate·d) for MCS at TAN of 7 g/L]. This should be explained as higher temperature favors SAO reaction energetically (Hattori 2008). Regarding the duration of lag phase, initiation of SAO-HM in TCS and MCS took 49–54 d and 62–70 d, respectively; the recovery of AM activity in MFS took 64–77 d. This long lag phase should result from the slow growth of the ammonia-tolerant microorganisms performing SAO, HM or AM. As reported previously, the co-culture of syntrophic acetate oxidizing bacteria (SAOB) and hydrogenotrophic methanogens usually had a long doubling time of 9–78 d (Westerholm 2012). Growth of SAOB under thermophilic conditions was faster than that under mesophilic conditions; predominance of ammonia-tolerant Methanosarcinaceae, however, took a longer period. The even longer lag phase and lower reaction rate for MCS and MFS at TAN of 9 g/L indicated that quite high ammonia concentration can also inhibit SAOB and ammonia-tolerant Methanosarcinaceae, which was reported by Lü *et al.* (2013).

This study suggested that stable performance can be obtained via SAO-HM pathway in biogas reactors operated at high ammonia concentrations (up to 1.2 g/L of $NH_3$ and 9 g/L of TAN). Since the growth and reaction rate of the functional microorganisms under high-ammonia conditions are much slower than the acetotrophic methanogens growing at lower-ammonia levels, a long hydraulic retention time (HRT) (>50 d) is required to maintain the dominance of these microorganisms, and the biogas production rate is lower compared with that of the AM-dominated reactors. Besides the SAOB, some members of Methanosarcinaceae can also prevail under such conditions as observed in the mesophilic MFS and previous studies (Fotidis *et al.* 2013a; Lü *et al.* 2013; Hao *et al.* 2015). The AM activity of these microbes was even higher than that of acetate-oxidizing syntrophs at similar conditions. Factors influencing the competition between SAOB and Methanosarcinaceae under high ammonia concentrations are still not clear. Temperature may play some role, since thermophilic operation seems to favor the growth of SAOB, as indicated by the higher methane production rate and shorter lag period under this condition. It is also demonstrated that, when $NH_3$ concentration reached 200 mg/L, the operation of the anaerobic digesters should be re-examined and adjusted to improve the establishment of ammonia-tolerant microbial communities. HRT and temperature should be particularly considered, as well as the mixing conditions which may influence the contact between SAOB and the hydrogenotrophs.

## CONCLUSIONS

Methane production pathways and their specific rates were studied at TAN concentrations of 0.14–9 g/L in acetate-fed biogas reactors inoculated with three methanogenic sludges. High levels of TAN showed significant inhibition of methanogenesis. This could, however, be recovered via SAO coupled with HM performed by acetate oxidizing syntrophs or through Acetoclastic Methanogenesis catalyzed by Methanosarcinaceae, after a long lag phase >50 d. $NH_3$ was the active component for this inhibition, of which 200 mg/L is suggested as a threshold for the shift of predominant pathway to SAO-HM. Methane production rate via SAO-HM at TAN of 7–9 g/L was about 5–9-fold lower than that of AM performed at TAN of 0.14 g/L, which was also lower than that of AM recovered at TAN of 7 g/L. Thermophilic condition favored the establishment of SAO-catalyzing microbial community, as indicated by the higher reaction rate and shorter lag phase. The operational strategy is thus suggested to be adjusted when $NH_3$ exceeds 200 mg/L, regarding HRT, temperature and mixing conditions.

## ACKNOWLEDGEMENTS

The experimental work was performed using scientific equipment acquired with the support DRRT Ile de France in the framework of the CPER-LABE (2007–2013) contract. The research is partially supported by the China National Science Foundation (Nos 51622809, 51378375) and China 111 Project. We also thank Chrystelle Bureau, Angéline Guenne, Lénaïck Rouillac, Nadine Derlet and Céline Madigou for their assistance during the analytical work.

## REFERENCES

Anthonisen, A. C., Loehr, R. C., Prakasam, T. B. & Srinath, E. G. 1976 Inhibition of nitrification by ammonia and nitrous acid. *J. Water Pollut. Control. Fed.* **48** (5), 835–852.

Chapleur, O., Bize, A., Serain, T., Mazéas, L. & Bouchez, T. 2014 Co-inoculating ruminal content neither provides active hydrolytic microbes nor improves methanization of $^{13}C$-cellulose in batch digesters. *FEMS Microbiol. Ecol.* **87**, 616–629.

Chen, Y., Cheng, J. J. & Creamer, K. S. 2008 Inhibition of anaerobic digestion process: a review. *Bioresour. Technol.* **99** (10), 4044–4064.

Demirel, B. & Scherer, P. 2008 The roles of acetotrophic and hydrogenotrophic methanogens during anaerobic conversion of biomass to methane: a review. *Rev. Environ. Sci. Biotechnol.* **7** (2), 173–190.

De Vrieze, J., Hennebel, T., Boon, N. & Verstraete, W. 2012 *Methanosarcina*: the rediscovered methanogen for heavy duty biomethanation. *Bioresour. Technol.* **112** (0), 1–9.

De Vrieze, J., Saunders, A. M., He, Y., Fang, J., Nielsen, P. H., Verstraete, W. & Boon, N. 2015 Ammonia and temperature determine potential clustering in the anaerobic digestion microbiome. *Water Res.* **75** (0), 312–323.

Fotidis, I. A., Karakashev, D., Kotsopoulos, T. A., Martzopoulos, G. G. & Angelidaki, I. 2013a Effect of ammonium and acetate on methanogenic pathway and methanogenic community composition. *FEMS Microbiol. Ecol.* **83** (1), 38–48.

Fotidis, I. A., Karakashev, D. & Angelidaki, I. 2013b Bioaugmentation with an acetate-oxidising consortium as a tool to tackle ammonia inhibition of anaerobic digestion. *Bioresour. Technol.* **146**, 57–62.

Fujishima, S., Miyahara, T. & Noike, T. 2000 Effect of moisture content on anaerobic digestion of dewatered sludge: ammonia inhibition to carbohydrate removal and methane production. *Water Sci. Technol.* **41** (3), 119–127.

Hao, L. P., Lü, F., Mazéas, L., Desmond-Le, Q. E., Madigou, C., Guenne, A., Shao, L. M., Bouchez, T. & He, P. J. 2015 Stable isotope probing of acetate fed anaerobic batch incubations shows a partial resistance of acetoclastic methanogenesis catalyzed by *Methanosarcina* to sudden increase of ammonia level. *Water Res.* **69**, 90–99.

Hao, L., Bize, A., Conteau, D., Chapleur, O., Courtois, S., Kroff, P., Desmond-Le Quéméner, E., Bouchez, T. & Mazéas, L. 2016 New insights into the key microbial phylotypes of anaerobic sludge digesters under different operational conditions. *Water Res.* **102**, 158–169.

Hattori, S. 2008 Minireview: syntrophic acetate-oxidizing microbes in methanogenic environments. *Microbes. Environ.* **23** (2), 118–127.

Karakashev, D., Batstone, D. J., Trably, E. & Angelidaki, I. 2006 Acetate oxidation is the dominant methanogenic pathway from acetate in the absence of *Methanosaetaceae*. *Appl. Environ. Microbiol.* **72** (7), 5138–5141.

Leite, A. F., Janke, L., Harms, H., Richnow, H.-H. & Nikolausz, M. 2016 Lessons learned from the microbial ecology resulting from different inoculation strategies for biogas production from waste products of the bioethanol/sugar industry. *Biotechnol. Biofuels* **9** (1), 144.

Lü, F., Hao, L. P., Guan, D. X., Qi, Y. J., Shao, L. M. & He, P. J. 2013 Synergetic stress of acids and ammonium on the shift in the methanogenic pathways during thermophilic anaerobic digestion of organics. *Water Res.* **47**, 2297–2306.

Lv, Z., Hu, M., Harms, H., Richnow, H. H., Liebetrau, J. & Nikolausz, M. 2014 Stable isotope composition of biogas allows early warning of complete process failure as a result of ammonia inhibition in anaerobic digesters. *Bioresour. Technol.* **167**, 251–259.

Narihiro, T., Nobu, M. K., Kim, N. K., Kamagata, K. & Liu, W. T. 2015 The nexus of syntrophy-associated microbiota in anaerobic digestion revealed by long-term enrichment and community survey. *Environ. Microbiol.* **17** (5), 1707–1720.

Qu, X., Mazéas, L., Vavilin, V. A., Epissard, J., Lemunier, M., Mouchel, J. M., He, P. J. & Bouchez, T. 2009 Combined monitoring of changes in delta$^{13}CH_4$ and archaeal community structure during mesophilic methanization of municipal solid waste. *FEMS Microbiol. Ecol.* **68** (2), 236–245.

Schnürer, A. & Nordberg, A. 2008 Ammonia, a selective agent for methane production by syntrophic acetate oxidation at mesophilic temperature. *Water Sci. Technol.* **57** (5), 735–740.

Sun, L., Müller, B., Westerholm, M. & Schnürer, A. 2014 Syntrophic acetate oxidation in industrial CSTR biogas digesters. *J. Biotechnol.* **171**, 39–44.

Vaughn, L. J. S., Conrad, M. E., Bill, M. & Torn, M. S. 2016 Isotopic insights into methane production, oxidation, and emissions in Arctic polygon tundra. *Glob. Chang. Biol.* **22** (10), 3487–3502.

Werner, J. J., Garcia, M. L., Perkins, S. D., Yarasheski, K. E., Smith, S. R., Muegge, B. D., Stadermann, F. J., DeRito, C. M., Floss, C., Madsen, E. L., Gordon, J. I. & Angenent, L. T. 2014 Microbial community dynamics and stability during an ammonia-induced shift to syntrophic acetate oxidation. *Appl. Environ. Microbiol.* **80** (11), 3375–3383.

Westerholm, M. 2012 *Biogas Production Through the Syntrophic Acetate-Oxidising Pathway: Characterization and Detection of Syntrophic Acetate-Oxidising Bacteria*. PhD Dissertation, Swedish University of Agricultural Sciences. Uppsala, Sweden.

Westerholm, M., Dolfing, J., Sherry, A., Gray, N. D., Head, I. M. & Schnürer, A. 2011 Quantification of syntrophic acetate-oxidizing microbial communities in biogas processes. *Environ. Microbiol. Rep.* **3** (4), 500–505.

Whiticar, M. J., Faber, E. & Schoell, M. 1986 Biogenic methane formation in marine and freshwater environments: $CO_2$ reduction vs. acetate fermentation- isotopic evidence. *Geochim. Cosmochim. Acta* **50**, 693–709.

Wiegant, W. M. & Zeeman, G. 1986 The mechanism of ammonia inhibition in the thermophilic digestion of livestock wastes. *Agric. Wastes* **16** (4), 243–253.

Zinder, S. & Koch, M. 1984 Non-aceticlastic methanogenesis from acetate:acetate oxidation by a thermophilic syntrophic coculture. *Arch. Microbiol.* **138**, 263–272.

Zwietering, M. H., Jongenburger, I., Rombouts, F. M. & van't Riet, K. 1990 Modeling of the bacterial growth curve. *Appl. Environ. Microbiol.* **56** (6), 1875–1881.

First received 18 June 2016; accepted in revised form 9 January 2017. Available online 3 February 2017